Rituximab exposure is influenced by baseline metabolic tumor volume and predicts outcome of DLBCL patients: a Lymphoma Study.

Mira Tout, Olivier Casasnovas, Michel Meignan, Thierry Lamy, Franck Morschhauser, Gilles Salles, Emmanuel Gyan, Corinne Haioun, Mélanie Mercier, Pierre Feugier, et al.

Rituximab Exposure is Influenced by Baseline Metabolic Tumor Volume and Predicts Outcome of DLBCL Patients: A LYSA Study.

Mira Tout,[1] Olivier Casasnovas,[2] Michel Meignan,[3] Thierry Lamy,[4] Franck Morschhauser,[5] Gilles Salles,[6] Emmanuel Gyan,[7] Corinne Haioun,[8] Mélanie Mercier,[9] Pierre Feugier,[10] Sami Boussetta,[11] Gilles Paintaud,[1,12] David Ternant,[1,12] and Guillaume Cartron[13,14]

Affiliations

[1]Université François-Rabelais de Tours, CNRS, GICC UMR 7292, Tours, France;

[2]Department of Clinical Hematology, CHU Dijon, INSERM LNC UMR866, Dijon, France;

[3]LYSA Imaging, Henri Mondor University Hospital, Créteil, France;

[4]Department of Clinical Hematology, CHU Rennes, U917, Rennes 1 University, Rennes, France;

[5]Department of Clinical Hematology, CHU Lille, Unité GRITA, Université de Lille 2, Lille, France;

[6]Hospices Civils de Lyon, Université Claude Bernard Lyon-1, Department of Hematology, France;

[7]Department of Hematology and cell therapy, CIC INSERM U1415, CHU Tours, Tours, France;

[8]Lymphoid malignancies unit, Henri Mondor University Hospital, APHP and UPEC, Créteil, France;

[9]Department of Hematology, CHU Angers, Angers, France;

[10]Department of Hematology, CHU Nancy, Nancy, France;

[11]Lymphoma Academic Research Organisation, CHU Lyon-Sud, Lyon, France;

[12]CHU Tours, Laboratory of Pharmacology-Toxicology, Tours, France;

[13]Department of Hematology, CHU Montpellier, Montpellier, France;

[14]University of Montpellier, CNRS UMR 5235, Montpellier, France.

1

Corresponding author:

Guillaume Cartron, MD-PhD, Département d'Hématologie Clinique, Centre Hospitalier Régional Universitaire, 80 Avenue Augustin Fliche 34095 Montpellier Cedex 05, France. Phone: 33 (0) 4 67 33 83 64. Fax: 33 (0) 4 67 33 91 94. E-mail: g-cartron@chu-montpellier.fr.

Running head: $TMTV_0$, rituximab exposure and outcome in DLBCL

Abstract word count: 249/250 words

Text word count: 3461/4000 words

Number of tables and figures: 6

Reference count: 41

Key points

- Rituximab exposure decreased as metabolic tumor volume increased, and correlated with metabolic response and survival
- Rituximab dose could be individualized according to metabolic tumor volume to achieve optimal exposure and therefore optimal response

Abstract

High variability in patient outcome after rituximab-based treatment is partly explained by rituximab concentrations, and pharmacokinetic variability could be influenced by tumor burden. We aimed at quantifying the influence of baseline total metabolic tumor volume ($TMTV_0$) on rituximab pharmacokinetics and of $TMTV_0$ and rituximab exposure on outcome in patients with diffuse large B-cell lymphoma (DLBCL). $TMTV_0$ was measured by ^{18}F-FDG-PET/CT in 108 previously untreated DLBCL patients who received four 375 mg/m^2 rituximab infusions every 2 weeks in combination with chemotherapy in two prospective trials. A two-compartment population model allowed describing rituximab pharmacokinetics and calculating rituximab exposure (area under the concentration-time curve; AUC). The association of $TMTV_0$ and AUC with metabolic response after 4 cycles, as well as progression-free survival (PFS) and overall survival (OS), was assessed using logistic regression and Cox models, respectively. Cutoff values for patient outcome were determined using ROC curve analysis. Exposure to rituximab decreased as $TMTV_0$ increased (R^2=0.41, *P*<.0001). A high AUC in cycle 1 (≥9400 mg.h/L) was associated with better response (OR, 5.56; *P*=.0006) and longer PFS (hazard ratio [HR], 0.38; *P*=.011) and OS (HR, 0.17; *P*=.001). A nomogram for rituximab dose needed to

obtain optimal AUC according to $TMTV_0$ was constructed, and the 375 mg/m^2 classical dose would be suitable for patients with $TMTV_0$ <281 cm^3. In summary, rituximab exposure is influenced by $TMTV_0$ and correlates with response and outcome of DLBCL patients. Dose individualization according to $TMTV_0$ should be evaluated in prospective studies. Studies were registered at www.clinicaltrials.gov as NCT00498043 and NCT00841945.

1

INTRODUCTION

Rituximab is a chimeric anti-CD20 monoclonal antibody, approved for diffuse large B-cell lymphoma (DLBCL), follicular lymphoma, chronic lymphocytic leukemia, and rheumatoid arthritis. The initial dosing regimen of rituximab in patients with indolent non-Hodgkin's lymphoma, supported by two phase I dose-escalation trials,[1,2] was 375 mg/m^2 weekly for 4 consecutive weeks. From these studies, neither dose-response relationship nor dose-limiting toxicities were identified, and the reasons for selecting 375 mg/m^2 infusions remain unclear.[3] In studies of immunochemotherapy in DLBCL, rituximab was administered at the dose of 375 mg/m^2 often in 2- or 3-week schedules. Increasing the frequency of 375 mg/m^2 rituximab infusions did not result in better outcomes in all patients as compared to the classical regimen.[4] Thus dosing strategies independent of patients' characteristics might not be sufficient, and better strategies may consist in individualizing the dosing regimen.

As for most drugs, a standard dose of rituximab leads to highly variable clinical response, with few patients (6%) reaching complete remission as observed in the pivotal study.[5,6] This variability is partly explained by rituximab pharmacokinetic (PK) variability,[7–9] higher rituximab concentrations being associated with a better clinical response.[10–14] Target antigen burden is one of the potential sources of rituximab PK variability. The pivotal study in patients with recurrent low-grade lymphoma reported an inverse relationship between rituximab serum levels and both tumor volume and lymphocyte count at baseline.[8] In mice xenografted with human CD20-expressing tumor, rituximab clearance increased with tumor volume.[12] Hence, standard doses of rituximab and a high tumor volume may lead to low rituximab serum concentrations resulting in an insufficient therapeutic response. Rituximab population

pharmacokinetics was previously assessed in patients with DLCBL,[13,14] but the influence of tumor burden has never been investigated in these patients despite clinical evidence suggesting worse outcome in those exhibiting bulky tumor.[15,16]

The objectives of the present study were therefore to quantify the impact of total metabolic tumor volume ($TMTV_0$) measured on baseline using FDG-PET/CT on rituximab pharmacokinetics, concentration-response relationship, and prognosis in DLBCL patients treated with standard doses of rituximab, and to propose an individual rituximab dose adjustment according to baseline $TMTV_0$.

1

PATIENTS AND METHODS

Patients and treatment

Rituximab pharmacokinetic and clinical response data were obtained from two prospective, multicenter, randomized studies, LNH2007-3B and GOELAMS 02.03, conducted by formerly GELA and GOELAMS groups (recently merged as LYSA group). These studies were approved by ethical committees and were registered on ClinicalTrials.gov as numbers NCT00498043 (LNH2007-3B) and NCT00841945 (GOELAMS 02.03). Briefly, eligible patients were aged 18-59 years and 18-75 years, respectively, with previously untreated and histologically proven $CD20^+$ diffuse large B-cell lymphoma (DLBCL; WHO classification), receiving a first-line treatment of rituximab in combination with chemotherapy. High risk patients with an age-adjusted international prognostic index (aaIPI) of 2 or 3 were eligible for the LNH2007-3B trial, whereas GOELAMS 02.03 study recruited patients with Ann Arbor stage I or II with a tumor mass < 7 cm. Patients were excluded if they had a diagnosis or history of other types of lymphoma or malignancies, HIV infection, or contra-indications to rituximab or drugs contained in the chemotherapy regimens. The aim of LNH2007-3B study was to evaluate the complete response rate according to ^{18}F-fluorodeoxyglucose-positron emission tomography-computed tomography (FDG-PET/CT) criteria after 4 cycles of R-ACVBP-14 (rituximab, doxorubicin, cyclophosphamide, vincristine, bleomycine, and prednisone) or R-CHOP-14 (rituximab, doxorubicin, cyclophosphamide, vincristine, and prednisone). The consolidation treatment was allocated based on centrally reviewed PET assessment after induction immunochemotherapy and patients received either consolidative immunochemotherapy or high-dose therapy.[17] In the GOELAMS 02.03 study, induction therapy consisted of 4 cycles of R-CHOP-14. If complete response

according to FDG-PET/CT after induction therapy was achieved, patients with modified IPI=0 were randomized to receive or not radiotherapy, whereas those with modified IPI≥1 received two additional R-CHOP-14. Patients in partial response received two additional R-CHOP-14 followed by radiotherapy.[18] In both studies, rituximab was administered as four infusions of 375 mg/m^2 repeated every 2 weeks in the induction phase. At the time of enrolment, all patients signed written informed consent and an additional informed consent specific for the pharmacokinetic protocol.

Rituximab concentrations

Blood samples for rituximab serum concentration measurements were collected just before and two hours after each rituximab infusion during the four cycles of induction treatment in both studies. Additional samples were drawn in the LNH2007-3B study in 30 patients of each arm on day 5 of each induction cycle, and on time of FDG-PET/CT after the 4th induction cycle (PET4). In the GOELAMS 02.03 trial, additional samples were drawn on day 21 or on the evaluation day of cycle 4, and on an additional day of cycles 1 and 4. Rituximab concentrations were measured using an enzyme-linked immunosorbent assay (ELISA) derived from the technique of Blasco et al.[19] The limit of detection was 0.06 mg/L and the lower and upper limits of quantification were 0.20 mg/L and 7.0 mg/L, respectively.

$TMTV_0$ measurement

FDG-PET/CT was performed before treatment. $TMTV_0$ was computed on a semiautomatic FDA approved software, Imagys (Keosys, Saint-Herblain, France). Lesions were identified by visual assessment with PET images scaled to a fixed SUV

(standardized uptake value) display and color table. $TMTV_0$ was obtained by summing metabolic volumes of all local (MTV_L) nodal and extranodal lesions. The 41% SUV_{max} threshold method was used for MTV_L computation, as recommended by European Association of Nuclear Medicine.[20] A volume of interest (VOI) was set around each lesion (node or organ involvement) as previously described.[21] Several VOIs could be drawn in bulky regions in case of heterogeneity in SUV distribution.[21] Bone marrow involvement was included in volume measurement only if there was focal uptake. Spleen was considered as involved if there was focal uptake or diffuse uptake higher than 150% of the liver background. This method was demonstrated to be highly reproducible between observers and centers even when different software were used.[22]

Evaluation of response to treatment

In the LNH20073B trial two PET examinations at mid (PET2) and end of induction (PET4) were required and scheduled 2 weeks after the second and 4th cycle of immunochemotherapy, respectively. In the GOELAMS 02.03 trial, PET was only performed after the fourth cycle of R-CHOP-14 (PET4). A blinded central review in real time of the PET images was organized using the positoscope network.[23] PET data were interpreted by at least 2 of 3 PET experts. PET were binary interpreted as positive or negative, as recommended by the IHP,[24] where positive residual uptake should be at least 25% higher than reference background. In both trials, the response to treatment was classified on PET4 as complete metabolic response (CMR) if PET4 was judged negative and non-CMR otherwise.

Pharmacokinetic modeling

Rituximab pharmacokinetics (PK) was assessed with a population approach using Monolix® 4.3.2 (Lixoft®, Orsay, France). As previously reported for rituximab PK,[13,25] a structural two-compartment model best described the concentration data (Supplemental Methods). Rituximab exposure was measured using area under the concentration-time curve (AUC), computed using individual pharmacokinetic parameters. The association between $TMTV_0$ and rituximab exposure was assessed. Several factors, including sex, age, body size, and $TMTV_0$, were tested as covariates on pharmacokinetic model parameters. In the multivariate analysis, significant covariates for $P < .01$ were retained in the model (Supplemental Methods).

Association between tumor volume, rituximab exposure, and patient outcome

Progression-free survival (PFS) was defined as the time from inclusion to progression, relapse or death from any cause. Overall survival (OS) was defined as the time from inclusion to death from any cause. PFS and OS were estimated using Kaplan-Meier analysis and compared between patient groups using the log-rank test. The influence of rituximab exposure on PET4 response, as well as on PFS and OS, was evaluated using logistic regression analysis and Cox proportional hazards regression models, respectively. $TMTV_0$, sex, IPI score (0-2 vs 3-4), age, and associated chemotherapy (CHOP vs ACVBP) were also assessed as predictors of outcome. Results from Cox regression and logistic regression analyses were internally validated using bootstrap procedure[26,27] generating a total of 100 replicates. Optimal threshold cutoff for prediction of PET4 response, PFS, and OS, was identified with receiver operating characteristic (ROC) curve analysis and validated using bootstrap analysis (1000 replicates). *P* values < .05 (2-sided test) were considered to indicate statistical significance in the univariate and multivariate

analyses. When variables were redundant, the most significant was kept in the multivariate analysis to avoid multicollinearity. Statistical analysis was conducted using R Software version 3.2.2 (R Foundation for Statistical Computing, Vienna, Austria) and survival analysis was conducted using SAS version 9.43 (SAS Institute Inc., Cary, NC).

Individualized rituximab dose estimation

Concentration-time profiles of the first induction cycle were computed based on individual PK parameters. Doses needed to obtain the optimal AUC were calculated for $TMTV_0$ ranging from 1 to 4340 cm^3.

1

RESULTS

Patients characteristics

Data on rituximab concentrations and $TMTV_0$ were available from 108 patients (89 in the LNH2007-3B trial and 19 in the GOELAMS 02.03 trial) who were included in the pharmacokinetic analysis (Figure 1; Table 1). Sixty-three patients (58%) were male, with a median [range] age of 49 years [19-68 years]. Patients in the LNH2007-3B trial had higher median $TMTV_0$ (461 cm^3; range, 17-4339 cm^3) as compared to GOELAMS 02.03 study (11.8 cm^3; range, 0.8-75.8 cm^3). Survival analysis was performed on the 108 patients assessed for PK (Figure 1). In 11 of these 108 patients, PET4 response was not evaluated, and thus 97 patients were included in the response analysis (Figure 1).

$TMTV_0$ correlated with rituximab exposure and elimination half-life

Rituximab elimination half-life ($T_{1/2}\beta$) was 45 days in a subject with median BSA, and increased with $TMTV_0$ (Spearman $R^2 = 0.64$; $P < 2.2x10^{-16}$; Figure 2A), ranging from 12.7 days for the lowest $TMTV_0$ of 0.8 to 83.8 days for the highest $TMTV_0$ of 4339 cm^3. An inverse correlation was found between $TMTV_0$ and rituximab exposure before second injection (AUC_1; Spearman $R^2 = 0.41$; $P = 8.1x10^{-14}$; Figure 2B).

Rituximab exposure correlated with PET4 response and survival

Optimal predictive AUC_1 cutoff using Youden index[28] was 9400 mg.h/L for both PFS and OS with areas under ROC curves (AUC ROC) of 0.70 (95% CI, 0.60-0.81; P = .0003) and 0.73 (95% CI, 0.61-0.85; P = .0002), respectively (Figures 2C,D). Sensitivity and specificity were 79% and 58% for PFS, and 89% and 56% for OS. Using Youden index, optimal predictive AUC_1 value for PET4 response was

estimated at 9600 mg.h/L, with sensitivity and specificity of 55% and 81% respectively (Figure 2E). An AUC_1 value of 9400 mg.h/L, identical to that for PFS and OS, resulted in sensitivity and specificity of 61% and 69% respectively. Thus the sum of sensitivity and specificity was only slightly different between these two AUC_1 cutoff values. Therefore, the AUC_1 of 9400 mg.h/L was used as optimal value for subsequent analyses for outcome and PET4 response. The median AUC_1 cutoff values obtained after bootstrap analysis were nearly identical to the 9400 mg.h/L optimal value derived from the original data set.

Complete metabolic response after four cycles of immunochemotherapy was 50.5% (49 of 97 patients). Compared with non-responders, CMR patients had significantly higher rituximab exposure before second cycle (AUC_1, 8733 vs 9743 mg.h/L; Mann-Whitney *P* = .001; Figure 2F). In the univariate logistic regression analysis, $AUC_1 \geq$ 9400 mg.h/L, higher age, lower $TMTV_0$, and IPI score of 0-2 were associated with better response with no significant influence of associated chemotherapy (Table 2). Since AUC_1 and $TMTV_0$ were correlated (Figure 2B), AUC_1 which was the most significant was selected for the multivariate analysis. In the multivariate analysis, IPI score, and chemotherapy did not influence response while AUC_1 (odds ratio [OR], 5.56; 95% confidence interval [CI], 2.19-15.62; *P* = .0006) and age (OR, 1.06; 95% CI, 1.02-1.10; *P* = .004) were the only factors associated with response (Table 2). Parameters of the final model were confirmed by the bootstrap procedure (Supplemental Table 2), which indicates the stability of the model. Age was however unable to discriminate between CMR and non-CMR patients (AUC ROC = 0.60; 95% CI, 0.49-0.72; *P* = .062).

With a median follow-up of 48 months (95% CI, 43-51), 4-year PFS was 76% and 4-year OS was 82%. Patients with an $AUC_1 \geq$ 9400 mg.h/L cutoff (n=55; 51%) had a

significantly better 4-y PFS (83% vs 62%; log-rank *P* = .011) and 4-y OS (94% vs 69%; log-rank *P* = .0016) than those with AUC_1 under the cutoff value (Figure 3). Univariate Cox regression analysis showed longer PFS for higher AUC_1, lower $TMTV_0$, and in women, and longer OS for higher AUC_1 (Table 3). No significant changes in OS or PFS were observed according to IPI or chemotherapy. Between AUC_1 and $TMTV_0$, AUC_1 was selected for multivariate analysis given the significant correlation between the two variables (Figure 2B). In the multivariate analysis, an AUC_1 ≥ 9400 mg.h/L was associated with longer PFS (hazard ratio [HR], 0.38; 95% CI, 0.17-0.83; *P* = .011) and OS (HR, 0.17; 95% CI, 0.05-0.60; *P* = .001). The proportional hazards assumption was satisfied in the final model for both PFS (*P* = .23) and OS (*P* = .58). Using the bootstrap validation procedure, the multivariate Cox analysis for PFS and OS included AUC_1 with nearly similar parameter estimates (Supplemental Tables 3 and 4).

Nomogram for dose individualization

Based on the final model simulations, the optimal dose (D_t) to administer to a patient according to individual $TMTV_0$ value and resulting in the optimal AUC_1 of 9400 mg.h/L can be written as: $D_t(mg/m^2) = 237.5 \times (TMTV_0)^{0.081}$ (Supplemental Results). For instance, the standard dose of 375 mg/m^2 is suitable for patients with $TMTV_0$ below 281 cm^3. For the median $TMTV_0$ value in the population of 313.5 cm^3 (median value in the present study), a dose of 378 mg/m^2 would be required to achieve optimal exposure. A patient with a $TMTV_0$ of 4339 cm^3 (highest value in this study) would require a dose of 468 mg/m^2 (Supplemental Table 5). Finally, if we applied individualized dosing, the total dose of rituximab administered in the first immunochemotherapy cycle in patients potentially underexposed ($TMTV_0$ > 281 cm^3,

n=56 of 97) would have been 23140 mg/m^2 instead of 21000 mg/m^2 (Supplemental Table 5), followed by the 375 mg/m^2 dose per cycle in subsequent cycles.

1

DISCUSSION

To our knowledge, this is the first study describing the influence of total metabolic tumor volume (TMTV) on rituximab pharmacokinetics and concentration-response relationship in patients with DLBCL. Patients with higher tumor burden had lower exposure to rituximab which was associated with worse clinical response and shorter survival. Based on initial TMTV, individualized rituximab dose leading to optimal exposure and thereby optimal outcome was then predicted.

Rituximab pharmacokinetics was satisfactorily described using a two-compartment model as in previous studies.[13,14,25,29–31] We observed a decrease in exposure to rituximab with increasing $TMTV_0$. Similarly, rituximab serum levels were previously shown to correlate inversely with tumor bulk at baseline in low grade lymphoma.[8] This may be explained by increased rituximab clearance related to its elimination by the target-antigen. Daydé et al[12] also demonstrated an increase in rituximab elimination with tumor increase in a murine model of disseminated lymphoma. This phenomenon was previously described for several monoclonal antibodies and is known as target-mediated drug disposition (TMDD).[31–34] In contrast to these results, we showed in the present study that higher $TMTV_0$ was associated with increased rituximab volumes of distribution without modifying clearance (Supplemental Results). This may be due to increased retention of rituximab by the tumor, followed, after treatment discontinuation, by a slower return of rituximab to the circulation. Indeed, this slower release with increasing $TMTV_0$ is confirmed by higher rituximab elimination half-life, reaching 12 weeks for $TMTV_0$ of 4339 cm^3. Median half-life was 6.4 weeks, a value longer than that reported in follicular lymphoma (~3 weeks[29]). Similarly, Muller et al[13] reported a prolonged rituximab terminal half-life of 5 weeks in

DLBCL. However, these authors did not investigate the potential influence of tumor volume on rituximab pharmacokinetics as a factor that might be responsible for this prolonged half-life.

In our study, patient outcome assessed by response after the fourth induction cycle (PET4), PFS, and OS, was associated with rituximab exposure, and improved outcome was observed for higher area under the concentration-time curve of induction cycle 1 (AUC_1). These findings are in agreement with other studies in which higher rituximab concentrations were found in responders in both indolent lymphoma[8,11] and aggressive lymphoma.[7,10] Igarashi et al[9] also observed a longer time to progression in patients with higher serum rituximab levels.

Tumor burden was previously shown to be associated with clinical outcome where $TMTV_0$ evaluated by ^{18}F-FDG-PET/CT was reported as an independent predictor of OS in DLBCL patients treated by immunochemotherapy, with shorter OS in the high TMTV group.[16] Similarly, Pfreundschuh et al[15] observed worse OS for DLBCL patients treated by immunochemotherapy exhibiting bulky tumor. In our study, we found that tumor burden explained a large part of the variability in rituximab exposure, $TMTV_0$ accounting for 41% of AUC_1 variability. Since higher exposure to rituximab is associated with improved outcome, $TMTV_0$ may be considered as a predictor of adequate exposure to rituximab.

Previous studies attempted to optimize rituximab treatment by testing different dosing regimens.[7,13,35] Higher frequency of 375 mg/m^2 rituximab infusions did not result in better outcomes in all patients as compared to the classical regimen.[4,36] The SEXIE-R-CHOP-14 study demonstrated that an increased rituximab dose of 500 mg/m^2 in elderly male patients resulted in improved outcome.[37] However, the same

dose might not be appropriate for all DLBCL patients. Rituximab efficacy is influenced by factors other than patients' sex. Our findings demonstrating a clear influence of tumor volume on rituximab pharmacokinetics, hence on patient outcome, as well as previous studies in line with ours, suggest the benefit of adapting rituximab dose to $TMTV_0$.

In the present study, we propose individualizing rituximab dose based on $TMTV_0$ in order to achieve optimal exposure and thereby improved outcome. Associations between rituximab AUC and response were significant for induction cycles 1, 2, and 3 (data not shown) with no significant differences between the corresponding AUC ROC. Hence, subsequent analyses were based on the earlier AUC of first cycle. An optimal predictive AUC_1 value of 9400 mg.h/L was used for clinical response, PFS, and OS. Rituximab dose allowing to achieve optimal exposure in a patient with a given $TMTV_0$ can be calculated as: $D_t(mg/m^2) = 237.5 \times (TMTV_0)^{0.081}$. For patients with the highest $TMTV_0$ of 4339 cm^3, an increase of 25% (468 mg/m^2) over the standard dose would then be necessary to reach the optimal exposure. The standard 375 mg/m^2 dose would be appropriate for patients with $TMTV_0$ of 281 cm^3. Median $TMTV_0$ in the present study was 313.5 cm^3 and 52% of patients ($TMTV_0$ > 281 cm^3) were potentially underexposed to rituximab. Previous studies in DLBCL[16,38–40] reported median $TMTV_0$ around 300 cm^3, indicating that more than 50% of patients had $TMTV_0$ higher than the 281 cm^3 value. Although these data were not all obtained in series of patients with the same characteristics or measured using the same techniques, this suggests that a considerable proportion of DLBCL patients would benefit from this dose individualization.

Doses > 375 mg/m^2 of rituximab given as monotherapy were previously evaluated in aggressive B-cell lymphoma, and the 500 mg/m^2 dose seemed to be well tolerated.[41]

A 500 mg/m^2 dose of rituximab in association with chemotherapy was not associated with increased toxicities in male patients in the SEXIE-R-CHOP-14 study. Safety of rituximab doses > 375 mg/m^2, administered with chemotherapy, particularly in patients with high tumor volume, remains however to be investigated. Furthermore, a dose of 500 mg/m^2 for all patients would lead to an overexposure of 100% of our patients, which would also induce an extra cost of 33% whereas this extra cost could be evaluated according to our nomogram to be a mean of 0.11% in our population (from -33% to +25% according to individual $TMTV_0$). Thus, dose adapted approaches would represent a better use of resources.

The proposed dose individualization of rituximab in the present study was done retrospectively. The benefit of this dosing strategy needs therefore to be confirmed in a prospective clinical trial testing the adaptation of rituximab dose according to patients' baseline metabolic tumor volume versus the standard dosing regimen.

Although the population included in our study is younger than the general DLBCL population, it is of high similarity with DLBCL population in terms of the metabolic tumor volume. For instance, previously reported median $TMTV_0$ values in DLBCL were around 300 cm^3,[16,39] very similar to the median value in our population.

Overall, this study is the first to quantify the influence of metabolic tumor volume on rituximab pharmacokinetics in patients with DLBCL. We showed that rituximab exposure decreased with increasing baseline tumor volume. Rituximab exposure was found to be predictive of response after induction treatment, OS, and PFS. Our work allowed to design a nomogram giving the optimal dose to administer according to individual $TMTV_0$. These results should lead to design of future clinical trials testing the benefit of individual adjustment of rituximab dose to $TMTV_0$.

Acknowledgments

Measurements of rituximab serum concentrations were carried out within the CePiBAc platform. CePiBAc was cofinanced by the European Union. Europe is committed to the region Centre with the European Regional Development Fund. This work was supported by the French Higher Education and Research Ministry under the program 'Investissements d'avenir' Grant Agreement: LabEx MAbImprove ANR-10-LABX-53-01. The authors thank Anne-Claire Duveau, Caroline Guerineau-Brochon, and Céline Desvignes for technical assistance, and Nicolas Azzopardi for pharmacokinetic advice.

This study was funded by GELA and GOELAMS groups and F. Hoffman-La Roche Ltd (Basel, Switzerland).

Disclosure

M Tout, M Meignan, T Lamy, M Mercier, P Feugier, and S Boussetta have no conflict of interest to disclose.

O Casasnovas received honoraria for participation in advisory boards organized by Roche, and received research funding from Roche.

F Morschhauser received honoraria for participation in advisory boards or scientific meetings organized by Roche.

G Salles received honoraria for participation in advisory boards or scientific meetings organized by Roche, and received a research grant from Roche.

E Gyan received research funding from Roche, is a coordinating investigator of a clinical trial supported by Roche, and received honoraria for scientific meetings organized by Roche.

C Haioun received honoraria for participation in advisory boards organized by Roche, and received research funding from Roche.

G Paintaud received research fundings from Novartis, Roche Pharma, Genzyme, MSD, Chugai and Pfizer, outside of the submitted work.

D Ternant has given lectures for Amgen and Sanofi.

G Cartron received consultancy fees and honoraria from Roche.

Author's contributions

M Tout collected, analyzed and interpreted data, performed pharmacokinetic and statistical analyses, and wrote the manuscript.

O Casasnovas designed research, collected data, analyzed and interpreted data, and wrote the manuscript.

M Meignan contributed study materials/patients, collected, analyzed and interpreted data, and wrote the manuscript.

T Lamy contributed study materials/patients, collected, analyzed and interpreted data, and reviewed the manuscript.

F Morschhauser contributed study materials/patients, collected, analyzed and interpreted data, and reviewed the manuscript.

G Salles contributed study materials/patients, collected, analyzed and interpreted data, and reviewed the manuscript.

E Gyan contributed study materials/patients, collected, analyzed and interpreted data, and reviewed the manuscript.

C Haioun contributed study materials/patients, collected, analyzed and interpreted data, and reviewed the manuscript.

M Mercier contributed study materials/patients, collected, analyzed and interpreted data, and reviewed the manuscript.

P Feugier contributed study materials/patients, collected, analyzed and interpreted data, and reviewed the manuscript.

S Boussetta collected, analyzed and interpreted data, performed statistical analysis, and reviewed the manuscript.

G Paintaud designed research, analyzed and interpreted data, and reviewed the manuscript.

D Ternant designed research, analyzed and interpreted data, and wrote the manuscript.

G Cartron designed research, contributed study materials/patients, collected, analyzed and interpreted data, and wrote the manuscript.

REFERENCES

1. Maloney D, Liles T, Czerwinski D, et al. Phase I clinical trial using escalating single-dose infusion of chimeric anti-CD20 monoclonal antibody (IDEC-C2B8) in patients with recurrent B-cell lymphoma. *Blood*. 1994;84(8):2457–2466.
2. Maloney DG, Grillo-lpez AJ, Bodkin DJ, et al. IDEC-C2B8□: results of a phase I multiple-dose trial in patients with relapsed non-hodgkin's lymphoma. *J. Clin. Oncol.* 1997;15(10):3266–3274.
3. Cartron G, Blasco H, Paintaud G, Watier H, Le Guellec C. Pharmacokinetics of rituximab and its clinical use: thought for the best use? *Crit. Rev. Oncol. Hematol.* 2007;62(1):43–52.
4. Murawski N, Pfreundschuh M, Zeynalova S, et al. Optimization of rituximab for the treatment of DLBCL (I): dose-dense rituximab in the DENSE-R-CHOP-14 trial of the DSHNHL. *Ann. Oncol.* 2014;25(9):1800–1806.
5. McLaughlin P, Grillo-López AJ, Link BK, et al. Rituximab chimeric anti-CD20 monoclonal antibody therapy for relapsed indolent lymphoma: half of patients respond to a four-dose treatment program. *J. Clin. Oncol.* 1998;16(8):2825–2833.
6. Grillo-López A. Rituximab (Rituxan/MabThera): the first decade (1993-2003). *Expert Rev. Anticancer Ther.* 2003;3(6):767–779.
7. Gordan LN, Grow WB, Pusateri A, et al. Phase II trial of individualized rituximab dosing for patients with CD20-positive lymphoproliferative disorders. *J. Clin. Oncol.* 2005;23(6):1096–1102.
8. Berinstein NL, Grillo-López A, White CA, et al. Association of serum Rituximab

(IDEC-C2B8) concentration and anti-tumor response in the treatment of recurrent low-grade or follicular non-Hodgkin's lymphoma. *Ann. Oncol.* 1998;9(9):995–1001.

9. Igarashi T, Kobayashi Y, Ogura M, et al. Factors affecting toxicity, response and progression-free survival in relapsed patients with indolent B-cell lymphoma and mantle cell lymphoma treated with rituximab: a Japanese phase II study. *Ann. Oncol.* 2002;13(6):928–943.

10. Tobinai K, Igarashi T, Itoh K, et al. Japanese multicenter phase II and pharmacokinetic study of rituximab in relapsed or refractory patients with aggressive B-cell lymphoma. *Ann. Oncol.* 2004;15(5):821–830.

11. Davis TA, White CA, Link B, et al. Single-agent monoclonal antibody efficacy in bulky non-hodgkin's lymphoma: results of a phase II trial of rituximab. *J. Clin. Oncol.* 1999;17(6):1851–1857.

12. Daydé D, Ternant D, Ohresser M, et al. Tumor burden influences exposure and response to rituximab: pharmacokinetic-pharmacodynamic modeling using a syngeneic bioluminescent murine model expressing human CD20. *Blood*. 2009;113(16):3765–3772.

13. Müller C, Murawski N, Wiesen MHJ, et al. The role of sex and weight on rituximab clearance and serum elimination half-life in elderly patients with DLBCL. *Blood*. 2012;119(14):3276–3284.

14. Blasco H, Chatelut E, Benz De Bretagne I, Congy-Jolivet N, Le Guellec C. Pharmacokinetics of rituximab associated with CHOP chemotherapy in B-cell non-Hodgkin lymphoma. *Fundam. Clin. Pharmacol.* 2009;23(5):601–608.

15. Pfreundschuh M, Ho AD, Cavallin-Stahl E, et al. Prognostic significance of

maximum tumour (bulk) diameter in young patients with good-prognosis diffuse large-B-cell lymphoma treated with CHOP-like chemotherapy with or without rituximab: an exploratory analysis of the MabThera International Trial Group. *Lancet Oncol.* 2008;9(5):435–444.

16. Sasanelli M, Meignan M, Haioun C, et al. Pretherapy metabolic tumour volume is an independent predictor of outcome in patients with diffuse large B-cell lymphoma. *Eur. J. Nucl. Med. Mol. Imaging*. 2014;41(11):2017–2022.

17. Casasnovas R-O, Meignan M, Berriolo-Riedinger A, et al. SUVmax reduction improves early prognosis value of interim positron emission tomography scans in diffuse large B-cell lymphoma. *Blood*. 2011;118(1):37–43.

18. Lamy T, Damaj G, Gyan E, et al. R-CHOP with or without Radiotherapy in Non-Bulky Limited-Stage Diffuse Large B Cell Lymphoma (DLBCL): Preliminary Results of the Prospective Randomized Phase III 02-03 Trial from the Lysa/Goelams Group. *56th ASH Annu. Meet. Expo.* 2014;124(21):92–5969.

19. Blasco H, Lalmanach G, Godat E, et al. Evaluation of a peptide ELISA for the detection of rituximab in serum. *J. Immunol. Methods*. 2007;325(1–2):127–139.

20. Boellaard R, Delgado-Bolton R, Oyen WJG, et al. FDG PET/CT: EANM procedure guidelines for tumour imaging: version 2.0. *Eur. J. Nucl. Med. Mol. Imaging*. 2015;42(2):328–354.

21. Meignan M, Sasanelli M, Casasnovas RO, et al. Metabolic tumour volumes measured at staging in lymphoma: methodological evaluation on phantom experiments and patients. *Eur. J. Nucl. Med. Mol. Imaging*. 2014;41(6):1113–

1122.

22. Kanoun S, Tal I, Berriolo-Riedinger A, et al. Influence of Software Tool and Methodological Aspects of Total Metabolic Tumor Volume Calculation on Baseline [18F]FDG PET to Predict Survival in Hodgkin Lymphoma. *PLoS One*. 2015;10(10):e0140830.

23. Meignan M, Itti E, Bardet S, et al. Development and application of a real-time on-line blinded independent central review of interim PET scans to determine treatment allocation in lymphoma trials. *J. Clin. Oncol.* 2009;27(16):2739–2741.

24. Juweid ME, Stroobants S, Hoekstra OS, et al. Use of positron emission tomography for response assessment of lymphoma: consensus of the Imaging Subcommittee of International Harmonization Project in Lymphoma. *J. Clin. Oncol.* 2007;25(5):571–578.

25. Ng CM, Bruno R, Combs D, Davies B. Population pharmacokinetics of rituximab (anti-CD20 monoclonal antibody) in rheumatoid arthritis patients during a phase II clinical trial. *J. Clin. Pharmacol.* 2005;45(7):792–801.

26. Efron B, Tibshirani R. Bootstrap Methods for Standard Errors, Confidence Intervals, and Other Measures of Statistical Accuracy. *Stat. Sci.* 1986;1(1):54–75.

27. Efron B. Bootstrap Methods: Another Look at the Jackknife. *Ann. Stat.* 1979;7(1):1–26.

28. Youden WJ. Index for rating diagnostic tests. *Cancer*. 1950;3(1):32–35.

29. Regazzi MB, Iacona I, Avanzini MA, et al. Pharmacokinetic behavior of rituximab a study of different schedules of administration for heterogeneous

clinical settings. *Ther. Drug Monit.* 2005;27(6):785–792.

30. Li J, Zhi J, Wenger M, et al. Population pharmacokinetics of rituximab in patients with chronic lymphocytic leukemia. *J. Clin. Pharmacol.* 2012;52(12):1918–1926.

31. Golay J, Semenzato G, Rambaldi A, et al. Lessons for the clinic from rituximab pharmacokinetics and pharmacodynamics. *MAbs*. 2013;5(6):826–837.

32. Panoilia E, Schindler E, Samantas E, et al. A pharmacokinetic binding model for bevacizumab and VEGF165 in colorectal cancer patients. *Cancer Chemother. Pharmacol.* 2015;75(4):791–803.

33. Hayashi N, Tsukamoto Y, Sallas WM, Lowe PJ. A mechanism-based binding model for the population pharmacokinetics and pharmacodynamics of omalizumab. *Br. J. Clin. Pharmacol.* 2007;63(5):548–561.

34. Gibiansky L, Sutjandra L, Doshi S, et al. Population pharmacokinetic analysis of denosumab in patients with bone metastases from solid tumours. *Clin. Pharmacokinet.* 2012;51(4):247–260.

35. Ternant D, Cartron G, Hénin E, et al. Model-based design of rituximab dosage optimization in follicular non-Hodgkin's lymphoma. *Br. J. Clin. Pharmacol.* 2012;73(4):597–605.

36. Pfreundschuh M, Poeschel V, Zeynalova S, et al. Optimization of rituximab for the treatment of diffuse large B-cell lymphoma (II): extended rituximab exposure time in the SMARTE-R-CHOP-14 trial of the german high-grade non-Hodgkin lymphoma study group. *J. Clin. Oncol.* 2014;32(36):4127–4133.

37. Pfreundschuh M, Held G, Zeynalova S, et al. Increased rituximab (R) doses and effect on risk of elderly male patients with aggressive CD20+ B-cell

lymphomas: Results from the SEXIE-R-CHOP-14 trial of the DSHNHL. *J. Clin. Oncol.* 2014;32(5s [suppl; abstr 8501]):

38. Kim J, Hong J, Kim SG, et al. Prognostic Value of Metabolic Tumor Volume Estimated by (18) F-FDG Positron Emission Tomography/Computed Tomography in Patients with Diffuse Large B-Cell Lymphoma of Stage II or III Disease. *Nucl. Med. Mol. Imaging (2010).* 2014;48(3):187–195.

39. Cottereau A-S, Lanic H, Mareschal S, et al. Molecular Profile and FDG-PET/CT Total Metabolic Tumor Volume Improve Risk Classification at Diagnosis for Patients with Diffuse Large B-Cell Lymphoma. *Clin. Cancer Res.* 2016;22(15):3801–3809.

40. Adams HJA, de Klerk JMH, Fijnheer R, et al. Prognostic superiority of the National Comprehensive Cancer Network International Prognostic Index over pretreatment whole-body volumetric-metabolic FDG-PET/CT metrics in diffuse large B-cell lymphoma. *Eur. J. Haematol.* 2015;94(6):532–539.

41. Coiffier B, Haioun C, Ketterer N, et al. Rituximab (anti-CD20 monoclonal antibody) for the treatment of patients with relapsing or refractory aggressive lymphoma: a multicenter phase II study. *Blood*. 1998;92(6):1927–1932.

FIGURE LEGENDS

Figure 1. Flow chart of patients included in the analysis. PET4, ^{18}F-FDG-PET/CT after the 4th induction cycle; and PK, pharmacokinetics.

Figure 2. Relationships between total metabolic tumor volume, rituximab pharmacokinetics, and patients' outcome. (A) Rituximab elimination half-life ($T_{1/2}\beta$) vs baseline total metabolic tumor volume ($TMTV_0$). (B) Rituximab exposure in induction cycle 1 (area under the concentration-time curve; AUC_1) vs $TMTV_0$. Receiver operating characteristic (ROC) curves of the predictive value of AUC_1 for (C) progression-free survival (PFS), (D) overall survival (OS), and (E) PET4 metabolic response. Corresponding areas under the ROC curves were 0.73, 0.70, and 0.69, respectively. (F) AUC_1 in complete metabolic responders (CMR) vs non-CMR (8733 vs 9743 mg.h/L; *P* = .001).

Figure 3. Kaplan-Meier estimates of (A) progression-free survival (PFS) and (B) overall survival (OS) by rituximab exposure in cycle 1 (AUC_1). Patients with $AUC_1 \geq 9400$ mg.h/L had significantly better 4-y PFS (83% vs 62%; log-rank *P* = .011) and 4-y OS (94% vs 69%; log-rank *P* = .0016) than those with $AUC_1 < 9400$ mg.h/L.

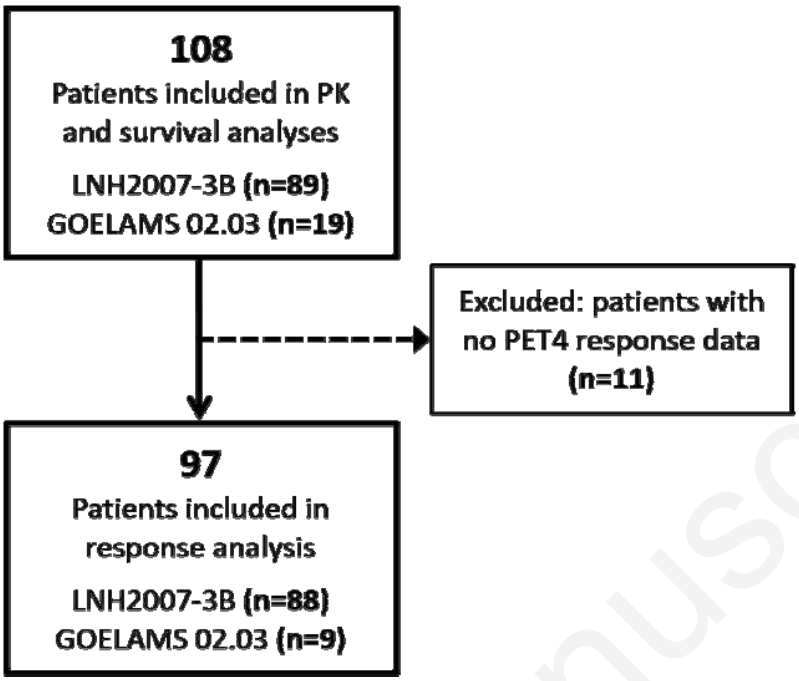

Figure 1

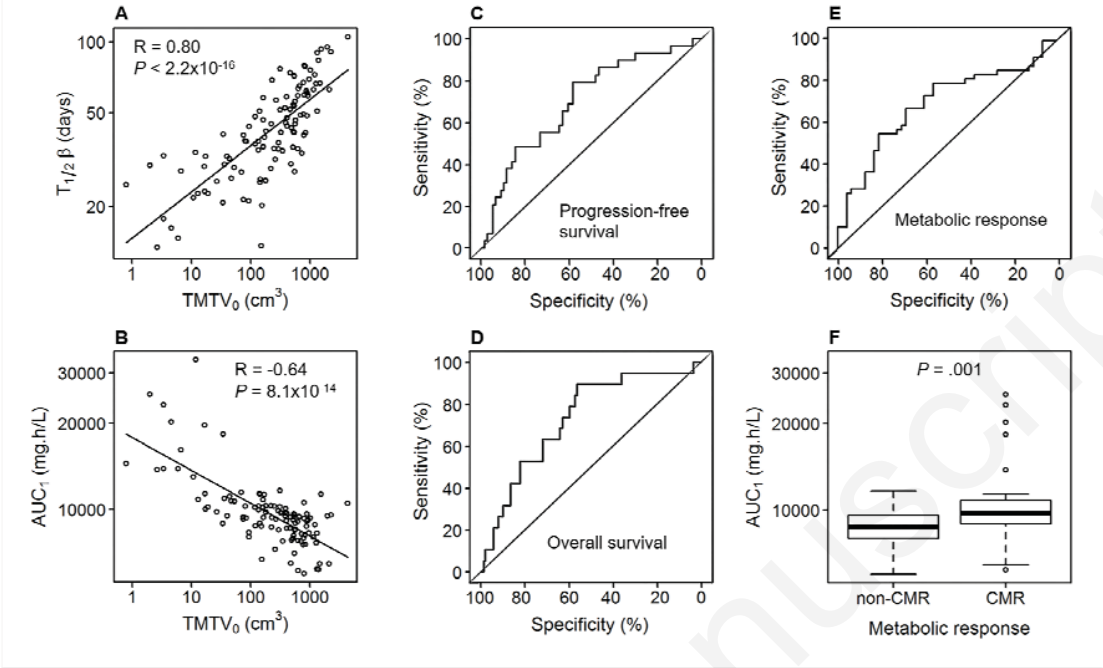

Figure 2

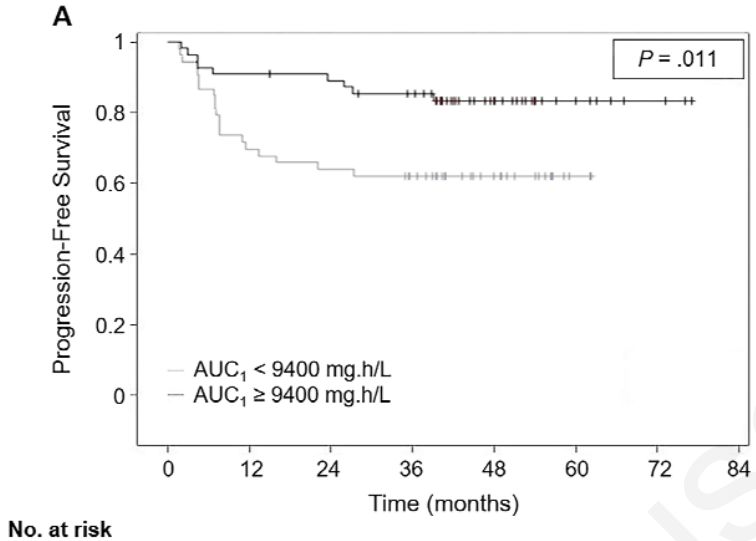

No. at risk

AUC_1 <9400	53	37	34	29	15	2	0
AUC_1 ≥9400	55	50	48	44	23	9	3	0

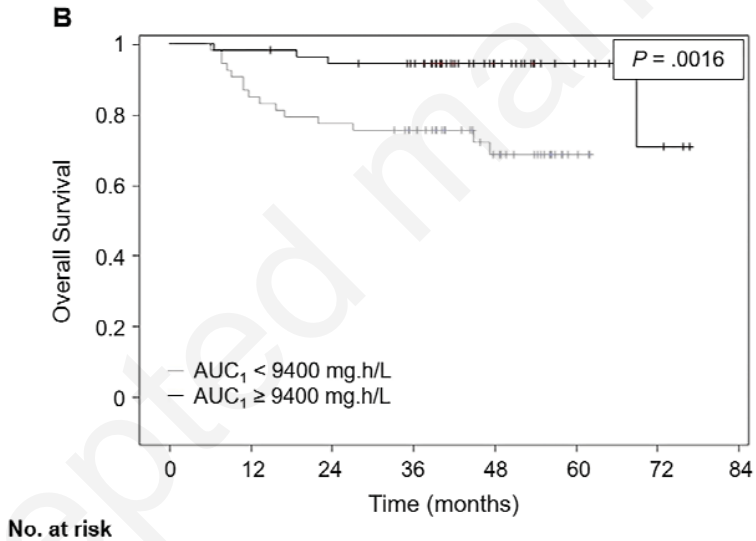

No. at risk

AUC_1 <9400	53	45	41	35	19	3	0
AUC_1 ≥9400	55	54	51	48	24	10	3	0

Figure 3

Table 1. Summary of patients' characteristics at baseline

Patients characteristics	LNH2007-3B (n=89)	GOELAMS 02.03 (n=19)	All
Sex : men/women, n	56/33	7/12	63/45
Age, years	47 [35-55]	54 [44-57]	49 [35-56]
Weight, kg	74 [63-83]	71 [58-80]	73.5 [63.0-82.2]
Body surface area, m^2	1.88 [1.74-2.03]	1.80 [1.65-1.88]	1.85 [1.68-2.00]
Ann Arbor stage, n (%)			
I/II	3 (3)	19 (100)	22 (20)
III/IV	86 (97)	0 (0)	86 (80)
IPI, n (%)			
0	0 (0)	15 (79)	15 (14)
1-2	29 (33)	4 (21)	33 (31)
3-4	60 (67)	0 (0)	60 (55)
Associated chemotherapy			
CHOP, n (%)	50 (56)	19 (100)	69 (64)
ACVBP, n (%)	39 (44)	0	39 (36)
$TMTV_0$, cm^3	461 [164-796]	11.8 [4.0-30.8]	313.5 [83.2-670.7]
Baseline lymphocytes, G/L	12.9 [7.3-21.0]	1.7 [1.4-2.0]	9.5 [4.0-16.9]
CMR, n (%)	41/88 (47)	8/9 (89)	49/97 (50.5)
AUC_1, mg.h/L	9497 [8920-10250]	16040 [10640-20940]	9743 [8967-10800]
Non-CMR, n (%)	47/88 (53)	1/9 (11)	48/97 (49.5)
AUC_1, mg.h/L	8730 [7973-9592]	9493	8733 [7989-9577]

Results are given as median [interquartile range]. ACVBP, doxorubicin, cyclophosphamide, vincristine, bleomycine, prednisone; AUC_1, rituximab area under the concentration-time curve before the second rituximab cycle; CHOP, rituximab, cyclophosphamide, doxorubicin, vincristine, and prednisone; CMR: complete metabolic responders; non-CMR: non complete metabolic responders; IPI, international prognostic index; and $TMTV_0$, baseline total metabolic tumor volume.

Table 2. Logistic regression analysis for predictors of response according to PET4 criteria in rituximab treated DLBCL patients (n=97).

	OR	95% CI	*P*
Univariate analysis			
AUC_1 ≥ 9400 mg.h/L	3.47	1.52-8.21	.004
$TMTV_0$, cm^3 ($x10^{-2}$)	0.91	0.82-0.98	.033
IPI (3-4)	0.36	0.15-0.82	.017
Chemotherapy (CHOP)	0.95	0.42-2.14	.90
Sex (male)	0.56	0.24-1.27	.17
Age, years	1.04	1.003-1.08	.036
Final model*			
AUC_1 ≥ 9400 mg.h/L	5.56	2.19-15.62	.0006
Age, years	1.06	1.02-1.10	.004

*Final model includes significant covariates in the multivariate analysis.

AUC_1, rituximab area under the concentration-time curve of the induction cycle 1; IPI, international prognostic index (0-2 vs 3-4); $TMTV_0$, baseline total metabolic tumor volume; OR, odds ratio; and 95% CI, 95% confidence interval.

Table 3. Cox regression analysis for PFS and OS in rituximab treated DLBCL patients (n=108).

	PFS			OS		
	HR	95% CI	*P*	HR	95% CI	*P*
Univariate analysis						
AUC_1 ≥ 9400 mg.h/L	0.38	0.17-0.83	.011	0.17	0.05-0.60	.001
$TMTV_0$, cm^3 ($x10^{-2}$)	1.07	1.02-1.13	.005	1.03	0.98-1.09	.24
IPI (3-4)	2.01	0.91-4.42	.082	2.14	0.76-6.00	.15
Chemotherapy (CHOP)	0.81	0.39-1.70	.577	1.09	0.41-2.90	.87
Sex (male)	2.42	1.03-5.66	.042	2.30	0.81-6.48	.11
Age, years	1.02	0.99-1.05	.262	1.03	0.99-1.08	.17
Final model with exposure*						
AUC_1 ≥ 9400 mg.h/L	0.38	0.17-0.83	.011	0.17	0.05-0.60	.001

*Final model includes significant covariates in the multivariate analysis.

AUC_1, rituximab area under the concentration-time curve of the induction cycle 1; HR, hazard ratio; IPI, international prognostic index (0-2 vs 3-4); OS, overall survival; PFS, progression-free survival; $TMTV_0$, baseline total metabolic tumor volume; and 95% CI, 95% confidence interval.